EasyChair Preprint

№ 14583

Evaluation of off-Road Uninhabited Ground Vehicle Mobility Using Discrete Element Method and Scalability Investigation

Ayush Nuwal, Ajay Kumar and Professor John Economou

August 28, 2024

7603 | Evaluation of off-road uncrewed ground vehicle mobility using discrete element method and scalability investigation

Ayush Nuwal [a,*], Ajay Kumar[b], John Economou[b]

[a] *Former Cranfield University PhD Student; currently at Bahrain Defence Force, General Headquarters, Bahrain*

[b] *Centre for Defence Engineering, Cranfield Defence and Security, Cranfield University, UK*

** Corresponding author: ajay.kumar@cranfield.ac.uk and Ayush.Nuwal@bdf.bh*

ABSTRACT

Modern armed forces are exploring the teaming of military vehicles with smaller uncrewed ground vehicles (UGVs), to improve the success of operations in complex and demanding off-road terrains. Smaller scale UGVs can be used to perform initial mobility testing on soft soils, to predict the go/no-go performance of larger crewed / uncrewed vehicles. Because of the variation in the sizes of the UGV and military vehicle, it is imperative whether the scalability of tyre-soil interaction exists or not. The scalability assumes that similar systems behave in a similar manner at different dimensional scales. Dimensional analysis is carried out to determine similarity between the systems and identify design parameters affecting scalability.

In this study, the lightweight vehicles (FED Alpha) are considered as the full-scale systems (as upper boundary) and UGVs (Husky or Warthog) as scaled system. The 335/65R22.5 tyre with operational range of loading for full scale vehicle is considered. The smaller UGV tyres (0.7, 0.5 and 0.25 scale) represent scaled system. The 2NS and fine-grain sands were modelled using the DEM (EpAM contact model). The direct shear and pressure-sinkage tests were simulated to calibrate the soil model (cone index from 14.79-149 kPa).

Validated simulations of tyre-soil interaction, show that 'drawbar-pull vs slip' and 'tractive-efficiency vs slip' are scalable, within given size and loading conditions. However, the prediction is dependent on soil parameters and size of the scaled systems (0.7 and 0.5 scale demonstrated the scalability clearly). The prediction was better in 2NS sand due to higher cone index. Up to 0.5 scale-system can predict the full- scale system's mobility performance on sandy soils. This result can be used to develop lighter UGVs to support full-scale vehicles in the off-road terrains.

Keywords
Scalability
Uncrewed Ground Vehicles
Mobility
Discrete Element Method

1. Introduction

Speed and mobility offer key tactical advantages to the armed forces on the battlefields. The rapid movement of mechanized land forces concentrated at the enemy's weak point often provides dominance on the modern battlefield. This is one of the popular military tactics in the history of warfare. Mechanized land warfare significantly depends on the use of infantry fighting vehicles, self-propelled artillery, and other combat vehicles, as well as other support units. However, climatic conditions and soil texture significantly challenge the vehicle mobility. Once the vehicle loses its ability to move and becomes immobile due to soil conditions or any other factors, then it becomes a vulnerable asset. Therefore, vehicle mobility in off-road conditions with suitable critical analysis can help to increase the vehicle mobility and therefore survivability.

With the advancements in modern military warfare, traditional mechanized land vehicles are now being integrated with autonomous systems. The NATO technical report highlights that there is a need for significant development to quantitatively model the mobility performance metrics of autonomous systems, particularly in the context of Uncrewed Ground Vehicles (UGVs) (NATO TR SAS – 097, 2018). UGVs are military robots that primarily operate off-road without human presence onboard, as depicted in Fig. 1. The increasing use of UGVs in present-day military operations, along with their expected greater deployment in the coming decades, raises questions about how to correlate the mobility of UGVs with that of full-scale military vehicles across various terrains and different climatic conditions encountered in NATO operations. As Science and Technology (S&T) continue to advance, future operating environments could become even more complex and uncertain, featuring high slippage areas, dense vegetation, or radioactive environments. Future UGVs capability can have the potential to significantly redefine the way modern warfare is conducted.

Fig. 1. REX UGV (Egozi, 2018)

Lower downside risk and higher confidence in the success of missions are two strong motivators for the continuous expansion of UGVs across a broad spectrum of warfighting and peacetime missions. During such missions, UGVs can team up with full-scale military vehicles to ensure three critical tasks as mentioned below.

- UGVs can be utilized for initial mobility testing on soft soil during missions to determine the go/no-go conditions for full-scale military vehicles. This capability would assist defense forces in preventing full-scale military vehicles from becoming immobilized during

https://doi.org/10.56884/ABCD1234 *(ed. note: ISTVS will update your paper's DOI)*
ISBN 978-1-942112-57-0

tactical operations on soft soils or off-road terrains, as depicted in Fig. 2. Furthermore, it would contribute to terrain mobility analysis, thereby improving its fuel economy and extending the operational vehicle range.

- Full-scale military vehicles frequently operate with heavy weapon systems and other heavy payloads on soft soils. The payload is a critical factor that significantly impacts mobility performance on soft soils. UGVs can be employed for initial mobility testing, allowing for the assessment of scaled payloads that simulate the conditions of full-scale vehicle payloads. Consequently, this will aid in determining the maximum payload carrying capacity of full-scale military vehicles on soft soils.
- Pre-planning the correct UGVs to team up with full-scale military vehicles for tactical operations is of utmost importance. The predictive capability of a UGV is essential for effectively monitoring and guiding the full-scale military vehicle, ensuring its safety while mitigating mission constraints such as no-go areas and communication limitations, and maximizing performance metrics such as speed and mobility. Therefore, the current study aims to facilitate the decision-making process for determining the suitable mobility specifications of supporting UGVs (e.g., tyre specifications and payload), scaled in accordance with full-scale military vehicles.

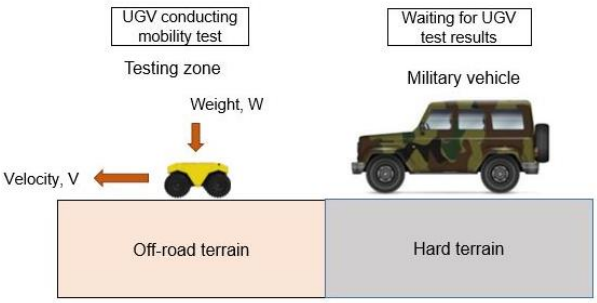

Fig. 2. UGV conducting initial mobility testing for the full-scale military vehicle to decide go/no-go condition on off-road terrain (or soft soils)

Historically, the assessment of wheeled vehicle mobility on off-road terrain has relied heavily on full-scale physical testing conducted in natural or prepared soil conditions. Over the past five decades, a significant portion of terramechanics research has focused primarily on light utility military vehicles, resulting in the development of various methodologies for predicting mobility. These methodologies have employed empirical approaches that involve resource-intensive and time-consuming experimental testing and have gained wide adoption within the defense research community (Jayakumar et al., 2013).

However, due to their empirical nature, it remains an open question whether the mobility performance models obtained from these methods can be used to accurately represent the mobility of small, lightweight Uncrewed Ground Vehicles (UGVs). Therefore, the concept of scalability in tyre-soil interaction is being proposed. Scalability is defined based on the assumption that it is possible to establish similar systems that exhibit similar behavior at different model scale (Freitag, 1966). Scale-model testing can be utilized to establish scalability in tyre-soil interaction system.

Further, to reduce the dependency on full-scale experimental testing, a novel simulation contact model using Discrete Element Method (DEM) has been implemented in EDEM software, to predict vehicle mobility based on vehicle and soil characteristics (DEM, 2011).

In the present study, the mobility analysis focuses on lightweight Armoured Personnel Carrier (APC) military vehicle tyres, such as the Land Rover (7.5R16) or FED Alpha tyre (335/65R22.5), as representative examples of full-scale systems. In contrast, the mobility analysis of small, lightweight UGVs considers tyres such as the Warthog (24'' Argo) as representative examples of scaled systems.

This paper is organized as follows. Section 2 discusses the scale model testing and establishes scalability in the context of the tyre-soil interaction system. Section 3 discusses the mobility performance parameters of the system. Section 4 uses the dimensional analysis technique to non-dimensionalise the performance parameters of the system. Section 5 discusses the discrete element method (DEM) simulation technique with the Edinburgh elastic-plastic adhesion (EpAM) contact model. Sections 6, 7 and 8 discuss the numerical simulation test procedure, results, and conclusion.

2. Scale model testing

Scale-model testing is an indispensable tool in the aerospace and shipbuilding industry. Small-scale modelling of full-scale aircraft and ships made it easy to address aerodynamics and hydrodynamics challenges over time within a controlled environment. It has proven useful in checking analytical work and providing empirical and semi-empirical solutions to challenges, which withstand the analytical treatment. The high costs of constructing and testing full-scale aircraft and ship models also made scale-model testing an economic necessity in both industries. Scale-model testing also provides the opportunity to perform controlled condition experiments, which are hazardous to operators while performing full-scale model testing. Aside from the economic benefits of small-scale model testing, it can solve immediate and specific technical problems. It is undoubtedly true in predicting changes in the full-scale model's mobility performance concerning design and environmental conditions using scale model testing. It can also yield design solutions to more complex challenges rapidly and economically.

Full-scale model testing has been the backbone of vehicle mechanics studies over the years. It is primarily, because of their relatively small size and ease of testing compared to aircraft and ships. Most of the past research focused on studying vehicle tyre interaction with uniformly prepared homogeneous soil test sections that incurred a substantial cost in order to generate an extensive database of the mobility performance parameters (e.g., drawbar pull vs slip, tractive efficiency) (Jayakumar et al., 2013). Therefore, scalability of tyre-soil interaction system can utilize the existing database of full-scale model testing to design and develop, cost-effective lighter UGVs to support full-scale military vehicles on the battlefield.

Swanson (1973) conducted scale model testing at the U.S. Army, Engineer Waterways Experiment Station (WES) to assess the tractive performance of different scale tyres on dual-layered terrain. The 2.50-4 tyre, representing a scale model that was approximately 1/5 times smaller than the full-scale standard military tyre, 11.00-20 of $2\frac{1}{2}$ ton truck, was chosen as the scale tyre for the tests. The experiments were performed on clay soil, considering two different cone index values: 160 kPa and 55 kPa. The scale tyre loading was varied between 111 N to 667 N with tyre deflection ranging from 15% and 35%. The experiments were performed at constant 20% slip for all tyre conditions. Fifteen

different combinations of wheel load, tyre deflection and soil strength were tested with three replications. It was found that sixty-eight percent of the mobility performance data of scale tyre was in the scatter band of 1-standard deviation of the full-scale tyre system. Therefore, the mobility performance of scale models follows normal distribution with respect to mobility performance of full-scale model.

Freitag (1966) performed the scale model testing on an approximately one-half scale model of full-scale tyre. It quotes "*The application of dimensional analysis to the experimental study of the vehicle-soil system is based on the fundamental assumption that similar systems that behave in a similar manner can be established. Thus, if the generalisations obtained by a systematic variation of the independent parameters are to be used with confidence, it must be shown that the observed tyre – soil relations do not vary with the size of the system*."

The 4.00-7 tyre, representing a scale model that was approximately 1/2 times smaller than the full-scale tyre, 9.00-14, was chosen as the scale tyre for the tests. Both tyres were tested at several different loads at several different loading conditions. The same forward speed was used for both tyres in all tests. Two types of similarities were established among both systems: Geometric similarity and dynamic similarity, using dimensional analysis. The geometric similarity ensures that both tyres have similar geometry while interacting with soil surface. It was achieved by keeping the same deflection number *(δ/h)* between the full-scale and scale systems. The dynamic similarity assures that the nature of interaction (e.g., transfer of forces and friction) is the same between the full-scale and scale systems. It was achieved by keeping the same clay loading number $\left(\frac{CI.d^2}{W}\right)$ between the full-scale and scale systems. It was found that the mobility performance parameters vs clay number datasets of the scale system were in close relation to the full-scale system curves.

Bekker (1956) proposed the use of dimensional analysis to develop an analytical model for the tyre-soil interaction system. This approach involves utilizing non-dimensional parameters to create similar systems. He introduced the concepts of geometric and dynamic similarity in tyre-soil interaction. Geometric similarity is achieved by equating the ratio of tyre physical parameters, such as tyre diameter to tyre width *(b/d)*, between the full-scale system and scale systems. Dynamic similarity is established when the full-scale system and prototype systems experience similar net forces.

However, in addition to performance parameters like drawbar pull force, Bekker identified separable force components that can interact with the tyre-soil interaction system. These components need to be considered in the analysis of the system. The stated force components are:

- Forces generated due to soil friction, cohesion (c) arising from the acceleration of the soil particles
- Forces from elastic deformation and viscous shearing of the soil
- Forces resulted from applied force and input torque
- Forces generated by soil to wheel friction

Bekker derived all the above separable force components into the non-dimensional group at the criterion of safe load as shown below. Ø is internal angle of friction, F is force term, l is length dimension and γ_s is specific weight.

$$(\emptyset, \frac{cl^2}{F}, \frac{\gamma_s l^3}{F})$$

Therefore, if the full-scale tyre and scale tyre are tested on the same soil model under identical soil conditions, it becomes possible to balance these non-dimensional parameters in both systems.

3. Tyre-soil interaction system

3.1. Mobility performance parameters

3.1.1. Longitudinal Slip Ratio (LSR)

Slip can be defined as the reduction in distance travelled or speed because of flexing in the tractive device (tyre or wheel) or shearing within the soil (R. He et al., 2020). It generally occurs between the overlapping surfaces of the tractive device and the terrain. The wheel slip ratio in the longitudinal direction of travel of the tractive device is considered as longitudinal slip ratio (LSR). The angle formed between the direction of travel and the line of intersection of the longitudinal central plane of tractive device is known as a slip angle (Wong, 2008). In this study, wheel slip ratio is defined as longitudinal slip ratio (LSR) at zero slip angle.

Mathematically, it can be defined as:

$$S = 1 - \frac{V_a}{\omega r} \quad (1)$$

where, S = Longitudinal slip ratio (LSR)
ω = angular velocity of the wheel, rad/s
r = rolling radius of the wheel on a hard surface, m
V_a = actual velocity of the wheel, m/s

3.1.2. Motion Resistance

In broad terms, motion resistance (MR) can be defined as the resistive force offered to the motion of a vehicle due to internal and external stimulus (R. He et al., 2020). The internal stimulus (R_{int}) is primarily due to the hysteresis developed into the tyre material because of carcass deflection and its impact inside the wheel or track while rolling. The external stimulus is an aggregate of compact resistance (R_c), bulldozing resistance (R_b), aerodynamic motion resistance (R_a), inertial resistance (R_i), slope resistance (R_s) and obstacle resistance (R_{ob}). The motion resistance is therefore given by Eq. 2.

$$MR = R_{int} + R_c + R_b + R_a + R_i + R_s + R_{ob} \quad (2)$$

3.1.3. Gross traction

Gross traction (GT) tends to be a thrust force generated due to powered wheel interaction with terrain (R. He et al., 2020). The powered wheel signifies a tyre with an input torque from the engine or motor. During this interaction, the powered running wheel applies force on the soil, trying to break it. Therefore, as per Newton's third law of motion, soil generates an equal and opposite force to wheel force. This opposite soil force generated is the thrust force or gross traction (GT). It helps the vehicle to overcome motion resistance and produce useful work.

3.1.4. Drawbar pull

Drawbar pull (D) is the excessive force produced by the vehicle at the drawbar to do the external work in the direction parallel to vehicle motion, as shown in Fig. 3 (R. He et al., 2020). Theoretically, drawbar pull defined as a difference of gross traction and motion resistance, as shown in Eq. 3. Hence, a positive drawbar pull indicates mobility, a zero pull indicates self-operation, and a negative pull indicates immobility.

$$D = GT - MR \quad (3)$$

3.1.5. Tractive efficiency

The term 'tractive efficiency' refers to the vehicle's capability in transforming the input axle power from the engine to the usable power available at the drawbar (R. He et al., 2020). Theoretically, it is defined as the drawbar power (P_d) available to the input power (P_{in}) by vehicle engine with sprocket torque, T and angular velocity of the drive wheel, ω as shown in Eq. 4. θ_r and θ_f are the rear and forward contact angles of the tyre-soil interface, as shown in Fig. 3. W is the normal load and N is the normal reaction force on tyre from surface.

$$\eta = \frac{P_d}{P_{in}} = \frac{D.V}{T.\omega} \tag{4}$$

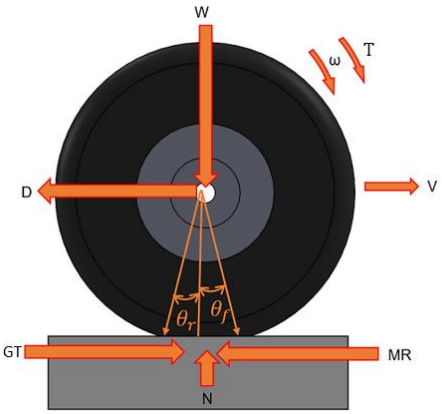

Fig. 3. Free body diagram of tyre-soil interaction system

3.2. Soil system

3.2.1. Cone Index

The cone index (CI), within the empirical methodology framework, is the most widely used mechanical property to determine soil strength. Experimentally, it is measured using a standard instrument known as cone penetrometer. A Cone penetrometer (Fig. 4) is a device, which has a conical surface or probe at its head with a tip downward and a cylindrical shaft as its body. A load cell (or dial indicator) is present at the top of the shaft within a proving ring, which indicates the force applied axially to the penetrometer. There are circumferential bands around the shaft that indicate the depth of penetration (R. He et al., 2020). The cone penetrometer's penetration velocity is kept slow and steady to maintain dynamic equilibrium to measure the cone index. This soil penetration resistance is the cone index. Theoretically, the cone index represents the force per unit base area that is necessary to push a cone probe into the soil at a steady rate.

Many of the existing empirical models use the cone index as a soil parameter to study soil's influence on vehicle mobility. This view is supported by the fact that the cone index profile is a composite property, reflecting both the soil's cohesive and frictional nature. However, it is difficult to separate the contribution from cohesion and friction between soil particles to soil's strength. Therefore, the cone index is used to analyze soil strength effect on the vehicle mobility in present study.

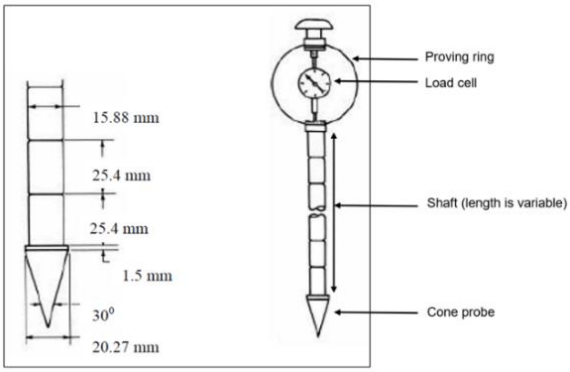

Fig. 4. Standard cone penetrometer (ASABE standard, 2006)

4. Dimensional analysis

Dimensional analysis is a powerful tool to reduce complex physical problems to the simplest form. In this approach, a non-dimensional relationship is developed by analyzing the fundamental dimensions of the physical parameters involved in the process. In this section, dimensional analysis is conducted on the mobility performance parameters of the tyre-soil interaction.

Tyre – soil interaction can be expressed as a function of nine independent variables as shown in Table 1 and three dependent variables as shown in Table 2 (Bekker, 1958; Freitag, 1966 and Swanson, 1973). However, the effect of the tyre's velocity is neglected by keeping it the same for both the full-scale and scale models testing (Freitag, 1966). Therefore, wheel torque, T can be expressed as a function of pertinent parameters shown in Table 1 and 2.

$$T = f(d, b, r, \delta, h, W, S, MR, D, CI) \tag{5}$$

Table 1
Independent variables

Parameter	Symbol	Dimension
Tyre diameter	d	L
Tyre width	b	L
Section height	h	L
Rolling radius	r	L
Tyre deflection	δ	L
Cone index	CI	$ML^{-1}T^{-2}$
Normal load	W	MLT^{-2}
Slip	S	-
Velocity	V	LT^{-1}

Table 2
Dependent variables

Parameter	Symbol	Dimension
Torque	T	ML^2T^{-2}
Motion resistance	MR	MLT^{-2}
Drawbar pull	D	MLT^{-2}

Using the Buckingham Pi theorem, the wheel torque, T can be written in nine functional Pi terms as shown in Eq. 6.

$$\frac{T}{rW} = \left\{\left(\frac{d}{r}\right), \left(\frac{b}{r}\right), \left(\frac{\delta}{r}\right), \left(\frac{h}{r}\right), (S), \left(\frac{MR}{W}\right), \left(\frac{D}{W}\right), \left(\frac{CI\,r^2}{W}\right)\right\} \tag{6}$$

The last Pi term $\left(\frac{CI.r^2}{W}\right)$ can be multiplied with $\left(\frac{d}{r}\right)$and $\left(\frac{b}{r}\right)$ Pi terms which are constant for any specific tyre at constant load.

Therefore, a more appropriate Pi term can be derived i.e., $\left(\frac{CI.b.d}{W}\right)$ which helps to understand the relationship between tyre-soil interaction. Therefore, equation 6 can be re-written as Eq. 7.

$$\frac{T}{rW} = \left\{\left(\frac{b}{d}\right), \left(\frac{r}{d}\right), \left(\frac{\delta}{h}\right), \left(\frac{h}{d}\right), (S), \left(\frac{MR}{W}\right), \left(\frac{D}{W}\right), \left(\frac{CI\ bd}{W}\right)\right\} \quad (7)$$

However, the relationship between dependent variables is as shown in Eq. 8.

$$\frac{MR}{W} = \frac{T}{rW} - \frac{D}{W} \quad (8)$$

The $\left(\frac{r}{d}\right)$ ratio is constant for most of the tyres at optimal inflation pressure, and thus, this term can be neglected in the tyre – soil interaction analysis. However, $\left(\frac{h}{d}\right)$ ratio between tyre parameters can be re-written as Eq. 9.

$$\frac{h}{d} = \frac{1 - \frac{2r}{d}}{\frac{\delta}{h}} \quad (9)$$

Therefore, the dependent parameters can be re-written, as shown below.

$$\frac{T}{rW} = f\left(\frac{b}{d}, \frac{\delta}{h}, S, \frac{CI\ bd}{W}\right) \quad (10)$$

$$\frac{D}{W} = g\left(\frac{b}{d}, \frac{\delta}{h}, S, \frac{CI\ bd}{W}\right) \quad (11)$$

where f and g are two different functions.

Therefore, all four Pi terms should be kept the same for similar systems. It governs the similar tyre-soil interaction for both full-scale and scale tyres. The Pi terms *(b/d)* should be the same during selection of scale tyre and full-scale tyre. The Pi term *(δ/h)* is the indicator of the stiffness of a tyre. It is also a function of tyre inflation pressure and tyre loading. As per the Engineering Design Handbook, automotive series, United States Army Material Command (1967) and Wong (2010) proposes that if the tyre inflation pressure is greater than the soil strength, then the tyre-soil contact area is round, and the tyre behaves like a rigid wheel. Moreover, the terrain deformation will be much greater than tyre deformation. Therefore, in this case, pneumatic tyre can be regarded as a rigid wheel (Wong, 2010).

The third Pi term is wheel slip. The mobility performance parameters are expressed as a function of wheel slip. Therefore, it is not considered a variable. The fourth Pi term ($\frac{CI\ bd}{W}$) contain the significant soil parameter, CI and the load, W. Both these parameters are independent variables and involves the concept of force. Therefore, for a constant tyre geometry, only changes in the cone index, CI and load, W can cause changes in the dependent variables. In this paper, the cone index was kept the same as both full-scale and scale tyres were tested on the same soil conditions.

Therefore, considering the tyre-soil interaction system based on tyre behaviour as rigid wheel and similar soil penetration consistency (or same soil conditions), the geometric and dynamic similarity criterion can be reduced to the term $\frac{W}{bd}$ which is the pressure term. However, the only pressure term acting in the tyre-soil interaction is the ground pressure. It is important to note that the average ground pressure is generated due to the transfer of forces from the tyre to the soil system. On equating the above parameter for full-scale and scale systems in the above conditions, the average ground pressure is the same for both systems. Therefore, similarity can be established between full-scale and scale tyre-soil systems by maintaining the same ground pressure term.

5. Discrete Element Method

5.1. Algorithm

Discrete Element Method (DEM) simulates the mechanical behaviour of a collection of arbitrarily shaped and arranged particles compromising in a system. A typical DEM material model schematic overview is shown in Fig. 5 (EDEM, 2011). It contains choice of particle shape, particle size distribution, particle parameters (e.g., particle density) and contact model. The particles act as independent entities and interact only at the contacts and interfaces between them. The algorithm involves the application of Newton's 2nd law of motion to particles and force-displacement law contact models at the interfaces. Newton's 2nd law of motion is used to determine the particle's motion arising from the contact and body forces on it. The force-displacement model is used to update the contact forces acting from each contact's relative motion.

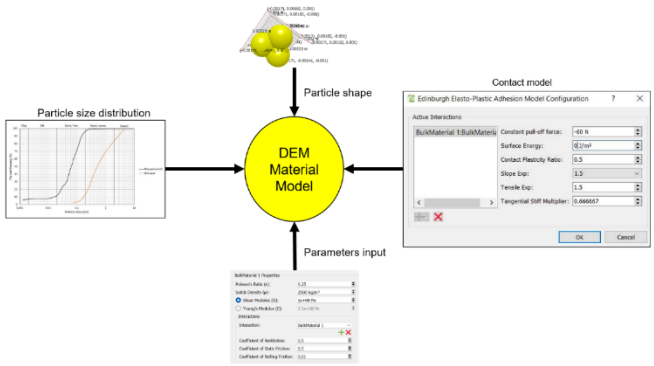

Fig. 5. A schematic overview of the DEM Material model (DEM, 2011)

The calculation cycle requires the repeated application of both the laws at each particle and relative contact, respectively, as shown in Fig. 6. Initially, the particles settle under gravity. The boundary condition is auto updated with the boundary of the box where the simulation takes place in the EDEM software as shown in Fig. 7. At the start of each cycle, the contacts are determined from the known particle positions. The force-displacement contact model is further applied to each contact to update the contact forces based on the relative motion, damping coefficient, and overlapping between the two entities at each time step, typically less than 1% of particle diameter. Later, the law of motion is applied to each particle to update its position and velocity based on the resultant forces and moments from the constitutive contact model and body forces acting on the particle. Further, the simulations were performed in the Altair EDEM software purchased under the academic license.

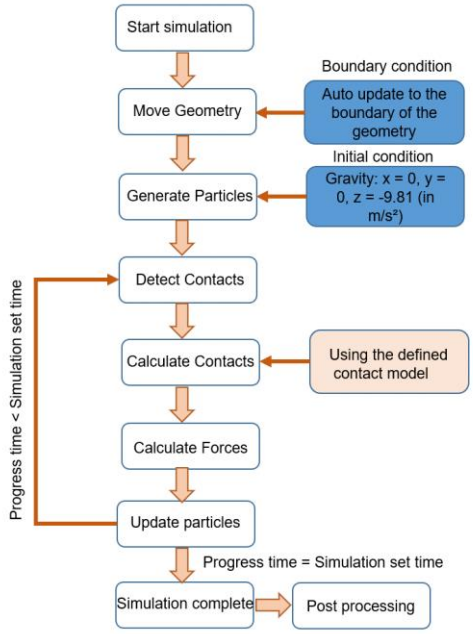

Fig. 6. Calculation cycle for DEM

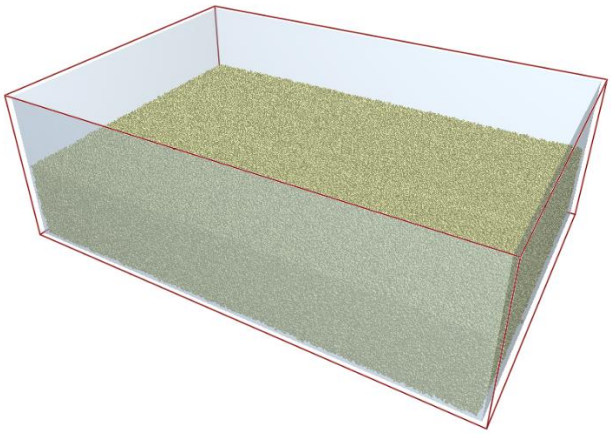

Fig. 7 Boundary condition of the box 6 m x 4 mx 2 m with red marking gets auto updated in Altair EDEM software

5.2. Edinburgh elastic-plastic adhesion contact model

The Edinburgh elastic-plastic adhesion (EpAM) contact model is based on the physics phenomenon observed in adhesive contacts between different nature and sizes of particles and entities. When two particles or entities are pressed together, they experience elastic and plastic deformation. It is assumed that the adhesive (or pull off) strength increases with an increase in the plastic contact area. Therefore, a non-linear contact model that accounts for both elastic and plastic deformation and contact area dependent adhesion is proposed. A schematic diagram of particle contact and normal force overlap *(f_n-δ)* curve for this model are in Fig. 8 (a) and (b).

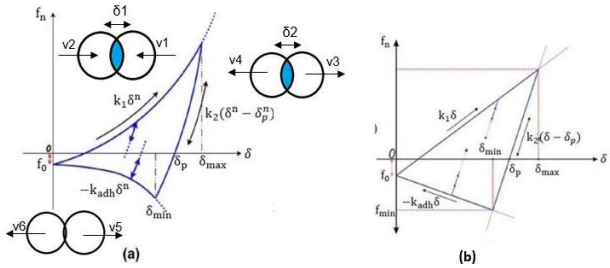

Fig. 8. EpAM normal force – displacement relationship (a) non-linear (b) linear (DEM, 2011)

The loading, unloading/reloading, and adhesive branches are characterised by seven parameters used in the model: the virgin loading stiffness parameter k_1, the unloading and re-loading stiffness parameter k_2, the contact plasticity ratio, λ_p, the constant adhesion force f_0, the adhesion energy parameter, $\Delta\gamma$, the adhesion exponent χ and the stiffness exponent n. The linearity and non-linearity of the loading and unloading branches are controlled by parameter n, and all becomes linear when n is equal to 1. The adhesion exponent χ controls the rate at which adhesion forces drop during contact separation; the higher the value, the sharper is the drop when plastically flattened contacts separate.

During the initial loading, the contact is determined using virgin loading path, k_1 and later, upon unloading of the contact; the contact switches to unloading/reloading path k_2, reaching zero force at a specific overlap which is also described as the plastic overlap, δ_p. If reloading occurs, then initially, the contact follows the unloading path k_2 but later switches to the virgin loading path k_1 when the previous maximum loading force is reached. Unloading along the k_2 path below the plastic overlap δ_p results in the maximum adhesive force development, f_{min} at $-f_0$-$k_{adh}\delta_{min}$. Further, unloading past this point reduces both the normal overlap and the attractive forces until the separation occurs at $\delta = 0$. If reloading of the contact occurs while on the adhesion branch, the contact follows the k_2 path (there are an infinite number of k_2 paths depending on the point of initial unloading) parallel to the initial unloading/reloading path until reaching the k_1 path. Further, loading takes place on the virgin loading path, k_1. When the particles are separated, the contact information is lost.

The default EDEM rolling friction model is based on a contact independent directional constant torque model. The total applied torque τ_i is given by Eq. 12.

$$\tau_i = -\mu_r f_{hys} R_i \omega_i \quad (12)$$

where, μ_r is the coefficient of rolling friction between two particles, and a particle and a wall. μ_r is the ratio of the rolling resistance force *(F)* and the normal reaction force *(N)*. R_i is the distance between the contact point and particle centre of mass and ω_i is the angular velocity at the contact point.

6. Numerical simulations

6.1. Soil data

Soil data represents the soil texture and strength parameters, which differentiate between types of soils. In the present study, two soil samples selected from the NATO NRMM CDT (2018). They are 2NS sand and fine-grained sand (FGS). Both sands are selected because of the availability of the soil test data (e.g., grain distribution, moisture content and bulk density).

2NS sand is a poorly graded medium sand but contains a fraction closer to the coarse sand (NATO CDT-308, 2020). It also has more angular sand particles. There are gravel particles in the sand, which makes it a little stiffer (Table 3). The fine-grained sand has cohesiveness due to the presence of silt and clay. It is sandy silt soil of low plasticity. Figure 9 shows the grain size distribution for both soils. The moisture content for 2NS sand is 1.13%, and FGS is 18.55%.

Two different soil models of 2NS sand and fine-grained soil of 6m x 4m x 2m were simulated using the EpAM contact model. The dimensions of the box were selected such that there is no boundary wall effect during the simulations. The models were validated using the experimental data of average cone index values of both sands. Table 3 shows the input parameters of the EpAM contact model. Further, the average cone index of 2NS sand is 149 kPa, and FGS is 22 kPa. The average bulk density of 2NS sand is 2687.66 kg/m^3, and FGS is 1466.64 kg/m^3.

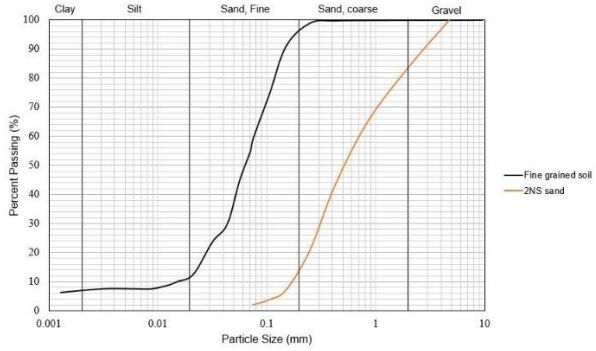

Fig. 9 Grain size analysis of 2NS sand and FGS (NATO CDT-308, 2020)

Table 3
Input simulation parameters of soil models

Input parameter	2NS sand	FGS
Particle density (kg/m3)	2500	2500
Particle size (mm)	10	10
Shear modulus, G (Pa)	5E+6	5E+8
Poisson's ratio, ϑ	0.4	0.25
Restitution, e	0.6	0.6
Static friction	0.5	0.5
Rolling friction	0.01	0.01
Constant pull off force, f_0 (N)	-60	-2
Surface energy $\Delta\gamma$ (J/m2)	0	7
Contact plasticity ratio λ_p	0.5	0.9
Slope exponent, n	1.5	1.5
Tensile exponent	1.5	1.5
Tangential stiffness multiplier, χ	0.67	0.67

6.2. Test tyre

The military vehicle, FED Alpha tyre (335/65R22.5), is considered a full-scale tyre (NATO CDT-308, 2020). The full-scale tyre is designated as Scale = 1. Figure 10 depicts the 3D CAD model of the exterior of the full-scale tyre, which was developed in SOLIDWORKS, v2018. The engineering datasheet from the Goodyear Technical Centre was utilized during the development process.

Fig. 10. Tyre model, 335/65R22.5

Additionally, three scaled prototypes of the full-scale tyre were constructed in SOLIDWORKS, with scaling factors of 0.7, 0.5, and 0.25. The scaling was done on geometrical dimensions (e.g., tyre diameter and width), while keeping the same non-dimensional parameter, tyre width/diameter *(b/d)* (Eq. 11). The tyre specifications of full-scale and scale tyres are shown in the Table 4.

Table 4
Tyre models specifications

Scale	d [mm]	b [mm]	r [mm]	Rim size	[b/d]
1	1011	335	505	22.5	0.33
0.7	708	234	354	16	0.33
0.5	505	167	253	11	0.33
0.25	253	84	126	5.5	0.33

Baranawoski et al. (2012) derived the tyre material properties experimentally to be used in the DEM modelling. The same material properties are used in the current study for all four tyres to ensure the same material stiffness. The tyre-soil interaction is defined using the EpAM contact model. Table 5 shows the input parameters for tyre model in DEM modelling.

Table 5
Input simulation parameters of tyre models

Input parameter	Value
Density (kg/m3)	1173
Shear modulus, G (Pa)	4.828E+06
Young's modulus, E (Pa)	14E+06
Poisson's ratio, ϑ	0.45
Restitution, e	0.6
Static friction	0.5
Rolling friction	0.01
Constant pull off force, f_0 (N)	0
Surface energy $\Delta\gamma$ (J/m2)	0.0045
Contact plasticity ratio λ_p	0.5
Slope exponent, n	1.5
Tensile exponent	1.5
Tangential stiffness multiplier, χ	0.67

6.3. Test procedure

Initially, the soil bin, a rectangular box of dimension 6 m long, 4 m wide and 4 m deep was generated for 2NS sand and FGS respectively. The soil particles (uniform angular shapes and sizes) were generated in this box and were allowed to settle under the gravity force till the kinetic energy of system becomes zero (Fig. 11). The particle size is upscaled to improve the simulation time and the discrete particle size does not significantly affect the simulation results. The mean particle size is kept constant, and scale of size variation was also kept constant to develop a homogeneous soil system. After settling, the thickness of soil bed

was 2 m, and 2 m high void region was provided above the soil bed surface so that the soil could flow without constraints (Fig. 7).

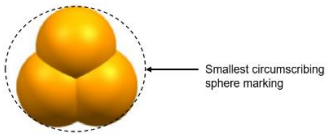

Fig. 11. 3D – 3 sphere particle model

A defined tyre model was imported into the EDEM software and was allowed to settle under gravity on the soil surface. A normal load was applied at the tyre center. Initially, the wheel was driven in a self-propelled condition, characterized by a longitudinal slip ratio of zero, where the circumferential velocity equals the wheel's translational velocity. This self-propelled condition was sustained for an initial duration of 0.5 seconds, during which no additional force was necessary to maintain the vehicle's current speed. In this state, a translational speed of 2.76 m/s and a rotational speed of 52.26 RPM (or 5.47 rad/s) were attained for the full-scale tyre model. The normal load of 13438 N was applied on the full-scale tyre model (NATO CDT-308, 2020).

Following the self-propelled condition, the wheel's rotational speed remained constant at 52.26 RPM (or 5.47 rad/s) for the full-scale tyre model. However, the translational speed was gradually decreased from its initial value of 2.76 m/s to zero over a period of 2 seconds. As a result, the slip varied from 0% to 100% over a duration of 2 seconds. Figures 12 and 13 show the full-scale tyre-soil interaction models.

However, the simulation procedure is similar to NATO CDT-308 (2020). However, in addition to that, this approach offers other advantages, such as maintaining a constant rotational speed and gradually reducing the translational speed. These benefits lead to a reduction in the distance traveled in the forward direction and also contribute to a decrease in computational time by reducing the number of test runs. Moreover, they have reduced the processing time from 10 days on a 6 GB RAM PC to 36 hours on 64 GB RAM PC.

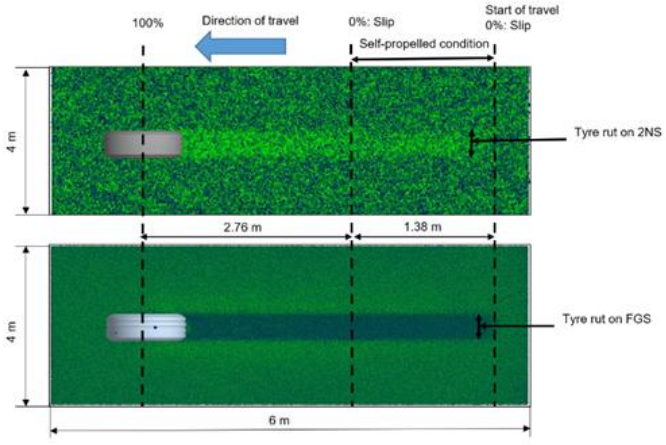

Fig. 12 Tyre testing procedure

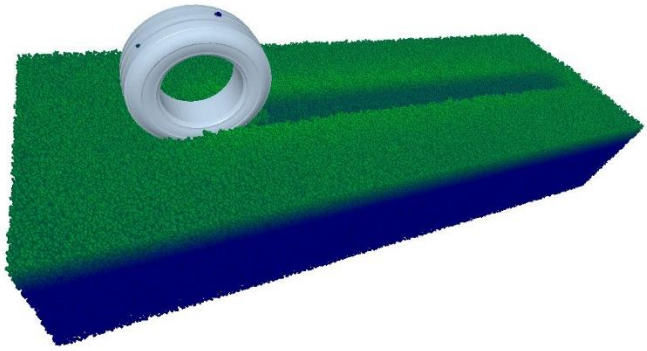

Fig. 13 3D model of Tyre-soil interaction system

A similar approach was adopted for the other three scaled tyres with scaling factors of 0.7, 0.5, and 0.25. The rotational speed of 52.26 RPM (or 5.47 rad/s) was maintained consistently for all tyres. Therefore, tyres have different initial translational speed to achieve respective self-propelled conditions. The normal loads on scale tyres were calculated by equating the pressure term $\frac{W}{bd}$ between the full-scale tyre system and scale tyre system as shown in Eq. 13. Table 6 shows the test matrix of full-scale and scale tyre models.

$$\left(\frac{W}{bd}\right)_{full-scale} = \left(\frac{W}{bd}\right)_{scaled} \tag{13}$$

Table 6
Test matrix

Scale	d [mm]	b [mm]	W [N]	[bd/W]
1	1011	335	13438	25.20
0.7	708	234	6585	25.20
0.5	505	167	3359	25.20
0.25	253	84	840	25.20

7. Results

7.1. Model validation

The full-scale tyre soil interaction model was validated with the experimental datasets of drawbar pull vs slip and NATO Reference Mobility Model (NRMM) (NATO CDT-308, 2020). Figures 14 and 15 compare the drawbar pull vs slip relation obtained from simulation model with the experimental datasets. The trend observed in the drawbar pull results aligns with previous studies conducted by Johnson et al. (2017) and Johnson et al. (2015), specifically in the case of a solid wheel operating on soft soil. A quantitative comparison between the simulation and experimental results revealed a mean error of 12% and 9% in the drawbar pull relationship for the 2NS sand and fine-grained sand models, respectively. The simulation results also fall within the prediction band of the NRMM model with an error of less than 10%. Therefore, the proposed simulation techniques, which employs the discrete element method with the Edinburgh elastic-plastic adhesion contact model, to accurately represent experimental conditions in software.

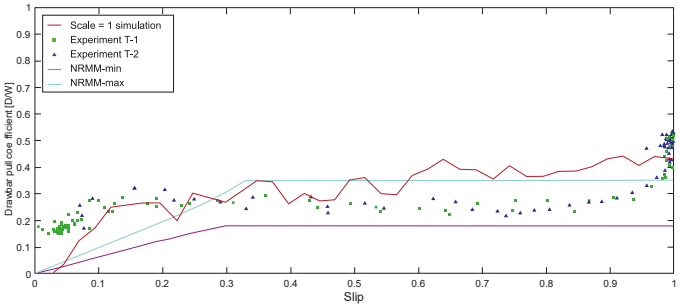

Fig. 14. Drawbar pull vs slip relation of full-scale tyre on 2NS sand

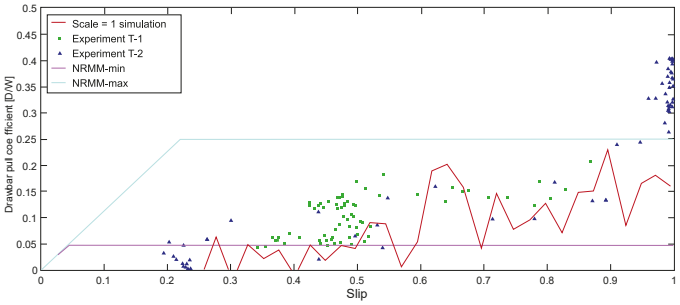

Fig. 15. Drawbar pull vs slip relation of full-scale tyre on FGS

7.2. Scalability analysis

Three independent parameters were incorporated to evaluate the mobility performance of powered-driven wheels. They are drawbar pull coefficient [D/W], gross traction coefficient [T/rW] and tractive efficiency [η]. Figures 16 to 18 shows the comparison of independent parameters of scale tyres (scale = 0.7, 0.5 and 0.25) with the full-scale tyre (scale = 1) on 2NS sand model. Figures 19 to 21 shows the comparison of independent parameters of scale tyres (scale = 0.7, 0.5 and 0.25) with the full-scale tyre (scale = 1) on FGS model. A one-standard-deviation scatter band, depicted using red dashed and star lines, was created around the datasets of the full-scale tyre. This scatter band serves to indicate the accepted error limits and facilitate the comparison of the datasets of the scaled tyres. Tables 7 and 8 present the percentage of data points from the scaled tyre systems (scale = 0.7, 0.5, and 0.25) that fall within the scatter band representing one standard deviation of the performance data points from the full-scale tyre (scale = 1).

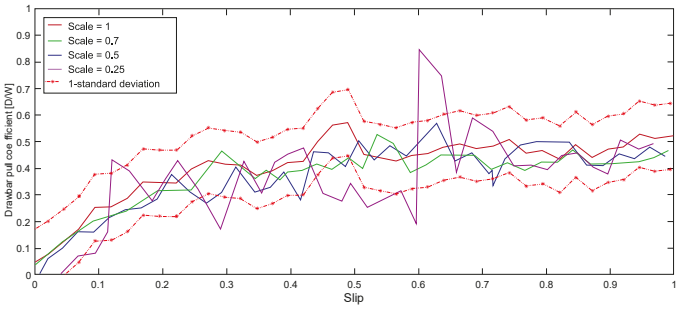

Fig. 16. Scalability of drawbar pull coefficient in 2NS sand

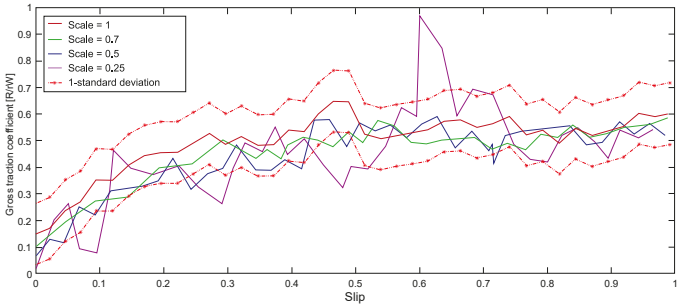

Fig. 17. Scalability of gross traction coefficient in 2NS sand

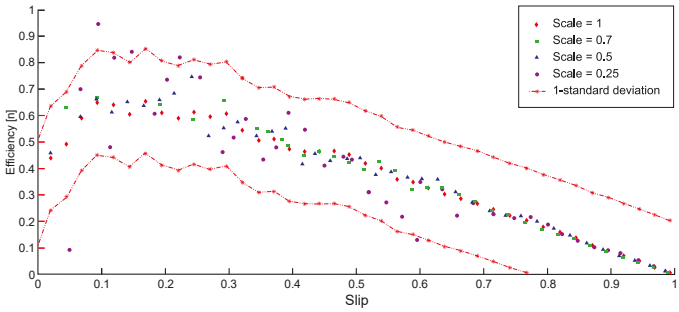

Fig. 18. Scalability of tractive efficiency in 2NS sand

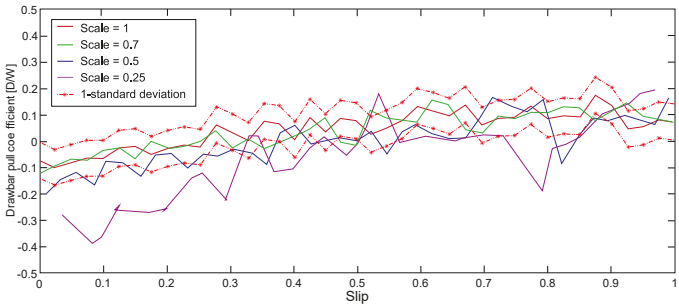

Fig. 19. Scalability of drawbar pull coefficient in FGS

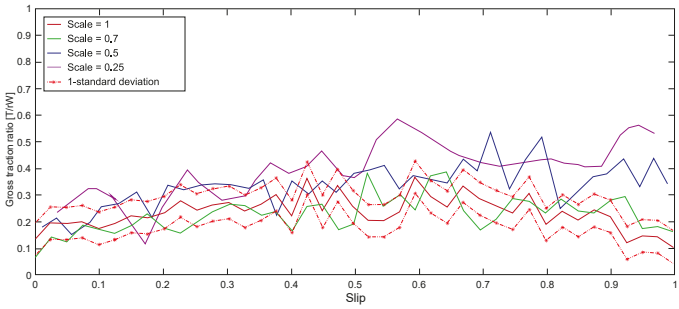

Fig. 20. Scalability of gross traction coefficient in FGS

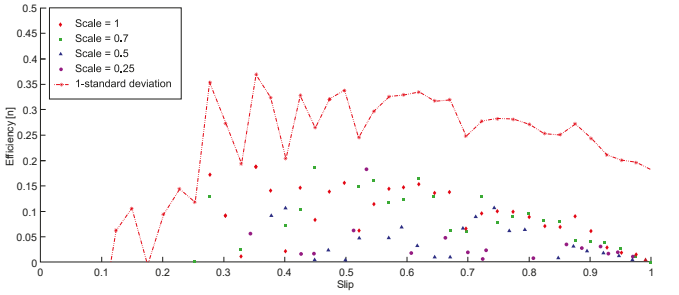

Fig. 21. Scalability of tractive efficiency in FGS

Table 7
Scalability analysis on 2NS sand

Scale	Parameter	Percentage (%)
0.7	D/W	100
	T/rW	97.1
	η	100
0.5	D/W	93
	T/rW	86.1
	η	97.7
0.25	D/W	75.6
	T/rW	80.5
	η	87.8

Table 8
Scalability analysis on FGS

Scale	Parameter	Percentage (%)
0.7	D/W	85.7
	T/rW	78.0
	η	63.4
0.5	D/W	70.7
	T/rW	41.4
	η	56.1
0.25	D/W	17.1
	T/rW	9.8
	η	41.5

The accuracy of scalability is better in 2NS sand than FGS. It might be due to the dependency of scalability on soil characterization and cone index. It was found that scale = 0.7 predicted better performance parameters of full-scale tyre system followed by scale = 0.5 and then by scale = 0.25 in both sands. It might be because of the increase in the rate of change of tyre curvature from 0.7 to 0.5 to 0.25 scaled tyre systems. The tyre curvature plays a significant role in predicting tyre-soil ground contact pressure/forces for tyre diameter less than 50 cm (Griffith and Spenko, 2011, 2013, 2014).

It can be seen that tractive efficiency is significantly affected by a decrease in the scale of tyres in FGS compared to 2NS sand. FGS is a low-bearing capacity soil with a lower cone index than 2NS sand. Therefore, it might be due to the increase in tailing pile build-ups in height (due to the digging effect) which increases the bulldozing resistance, as the scale reduces in FGS, thus reducing the drawbar pull (Fig. 19). There is a non-linear increase in tyre-soil contact area due to digging, which also increases the gross traction ratio (Fig. 20). Therefore, tractive efficiency is reduced in FGS with the scale.

8. Conclusion

The key findings of this study demonstrates that the scalability of tyre-soil system exists well in 2NS sand and Fine Grain Sand (FGS). The similarity between the different tyre-soil systems can be established by equating the pressure term, *(W/bd)*, for the same soil type. However, the accuracy of scalability decreases with the decrease in the scales of the tyre – soil systems. Up to 0.5 scale-system can predict the full- scale system's mobility performance on sandy soils. Furthermore, the accuracy depends on various factors such as the soil characterization, soil type and cone index.

According to the presented simulation technique, the discrete element method utilizing the Edinburgh elastic-plastic adhesion contact model (EpAM), provides a better prediction of the experimental drawbar pull versus slip relationship for the full-scale tyre on both soil types than NRMM. Therefore, the EpAM model can be utilized to design and optimize tyre performance on various soil types and improve our understanding of the tyre-soil interaction system.

Future research will investigate the applicability of scalability in heterogeneous soil models of 2NS sand and FGS. Further, the effect of parameters such as cone index, normal load and tyre deflection will be analysed.

9. Data Availability Statement

Experimental data supporting this study is openly available at https://www.mtu.edu/cdt/

10. References

ASABE Standards, 2006. ASAE S313.3 FEB04 Soil cone penetrometer. St. Joseph, Michigan, ASABE.

Baranowski, P., Bogusz, P., Gotowicki, P., Małachows, J., 2012. Assessment of mechanical properties of offroad vehicle tyre: coupons testing and - FE model development. Acta Mechanica et Automatica, 6(2), pp.17-22.

Bekker, M. G., 1956. Theory of land locomotion. The University of Michigan Press.

Bekker, M.G., 1969. Introduction to terrain-vehicle systems, vol. I. The University of Michigan Press.

DEM Solutions Ltd., 2011. EDEM 2.4 Theory Reference Guide. Edinburgh, Scotland, UK.

Egozi, A., 2018. US Army pursues Israeli robots. Breaking Defense, November 12. Available at: https://breakingdefense.com/2018/11/us-army-pursues-israeli-robots/ (Accessed: 2024.04.09).

Engineering Design Handbook, 1967. Automotive series, United States Army Material Command.

Freitag, D.R., 1965. A dimensional analysis of the performance of pneumatic tyres on soft soils. Technical report number: 3-688, USAE Waterways Experiment Station.

Griffith, M. G. and Spenko, M., 2011. A modified pressure–sinkage model for small, rigid wheels on deformable terrains. Journal of Terramechanics, 48 (2), pp. 149-155.

Griffith, M. G. and Spenko, M., 2013. A pressure-sinkage model for small-diameter wheels on compactive, deformable terrain. Journal of Terramechanics, 50(1), pp. 37-44.

Griffith, M. G. and Spenko, M., 2014. Development and experimental validation of an improved pressure-sinkage model for small-wheeled vehicles on dilative, deformable terrain. Journal of Terramechanics, 51, pp.19-29.

Jayakumar, P, Melanz, D, MacLennan, J, Gorsich, D, Senatore, C and Iagnemma, K, 2014. Scalability of classical terramechanics models for lightweight vehicle applications incorporating stochastic modeling and uncertainty propagation. Journal of Terramechanics, 54, pp. 37-57.

Johnson, B., Duvoy, X., Kulchitsky, V., Creager, C. and Moore, J., 2017. Analysis of Mars Exploration Rover wheel mobility processes and the limitations of classical terramechanics models using discrete element method simulations. Journal of Terramechanics, 73, pp. 61-71.

Johnson, B., Kulchitsky, V., Duvoy, P, Iagnemma, K, Senatore, C, Raymond, E. A. and Jeffery, M., 2015. Discrete element method simulations of Mars Exploration Rover wheel performance. Journal of Terramechanics, 62, pp. 31-40.

NATO CDT – 308, 2020. North Atlantic Treaty Organization STO Technical report Cooperative Demonstration of Technology (CDT- 308): Next-Generation NATO Reference Mobility Model (NG-NRMM), Research and Technology Organization.

NATO NRMM CDT, 2018. North Atlantic Treaty Organization STO Technical report AVT-248: Next-Generation NATO Reference Mobility Model (NRMM) Development, Research and Technology Organization.

NATO TR SAS – 097, 2018. North Atlantic Treaty Organization STO Technical report: AC/323 (SAS-097) TP/776, Research and Technology Organization.

Rui He, Corina Sandu, Hoda Mousavi, Mohit N. Shenvi, Kirsten Braun, Ray Kruger, P. Schalk Els, 2020. Updated Standards of the International Society for Terrain-Vehicle Systems, Journal of Terramechanics, Volume 91, 2020, Pages 185-231.

Swanson, G D, 1973. Scale-model Tyre Tests in clay. Journal of Terramechanics, 10 (3), pp. 21-27.

Wong J., 2008. Theory of ground vehicles, fourth ed., Wiley.

Wong, J., 2010. Terramechanics and Off-Road Vehicle Engineering, second ed., Wiley.